Transition-Metal Derivatives of Cyclopentadienylphosphine Ligands. 10. ((Cyclopentadienylethyl)diphenylphosphine)Rhodium and -iridium Chelated and Bridged Complexes: Crystal and Molecular Structures of the Chelated Complexes $(\eta^5{:}\eta^1\text{-}C_5H_4(CH_2)_2PPh_2)Rh^I(C_2H_4)$ and $(\eta^5{:}\eta^1\text{-}C_5H_4(CH_2)_2PPh_2)Rh^{III}I_2$

Inja Lee, Françoise Dahan, André Maisonnat, and René Poilblanc*

Laboratoire de Chimie de Coordination du CNRS, UPR 8241 lié par conventions à l'Université Paul Sabatier et à l'Institut National Polytechnique, 205 route de Narbonne, 31077 Toulouse Cedex, France

Received January 21, 1994®

A series of new derivatives of (cyclopentadienylethyl)diphenylphosphine—a heterodifunctional ligand able to offer either chelating or bridging properties—has been synthesized from various rhodium and iridium derivatives. Interestingly, the synthesis of the monometallic chelated carbonyl compound $(\eta^5{:}\eta^1\text{-}C_5H_4(CH_2)_2PPh_2)Rh(CO)$ (**8**) starting from the square-planar dimeric complex $[RhCl(CO)_2]_2$ and [((diphenylphosphino)ethyl)cyclopentadienyl]lithium involves a pathway beginning with coordination of the phosphorus moiety of the difunctional ligand. This pathway then includes the transient formation of *cisoid* and *transoid* isomers, **9a,b**, of the bridged dimetallic complex $[(\mu\text{-}\eta^5{:}\eta^1\text{-}C_5H_4(CH_2)_2PPh_2)Rh(CO)]_2$, as kinetic products which transform into the thermodynamic product **8**. A similar overall process is also suspected for the formation of the other chelated complexes-$(\eta^5{:}\eta^1\ C_5H_4(CH_2)_2PPh_2)M(C_2H_4)$ (M = Rh (**14**), Ir (**12**)) and $((\eta^5{:}\eta^1\text{-}C_5H_4(CH_2)_2PPh_2)M(cod)$ (M = Rh (**15**), Ir (**16**)), obtained from $[RhCl(C_2H_4)]_2$, $[IrCl(C_2H_4)]_n$, and $[MCl(cod)]_2$ (M = Rh, Ir), respectively. From **8** and **12** the chelated diiodo compounds $(\eta^5{:}\eta^1\text{-}C_5H_4(CH_2)_2\ PPh_2)M^{III}I_2$ (M = Rh (**17**), Ir (**18**)) were also synthesized. All of the more stable products (**8**, **12**, **14–18**) were fully characterized by their spectroscopic data (including phosphorus–rhodium coupling constant measurements) and by electron impact mass spectroscopy. Complex **14** crystallizes in the monoclinic space group $P2_1/n$ with eight molecules in the unit cell, the dimensions of which are a = 9.808(1) Å, b = 28.515(3) Å, c = 13.094(1) Å, β = 98.34(1)°, and V = 3623.3(8) Å^3. Least-squares refinement leads to a value for the conventional R index of 0.031 for 3035 reflections having $I > 3\sigma(I)$. Complex **17** crystallizes in the monoclinic space group $P2_1/n$ with four molecules in the unit cell, the dimensions of which are a = 10.439(1) Å, b = 16.557(2) Å, c = 11.458(1), Å, β = 95.85(1) Å, and V = 1970.1(8) Å^3. Least-squares refinement leads to a value for the conventional R index of 0.027 for 1638 reflections having $I > 3\sigma(I)$. In both compounds **14** and **17**, the P–C–C–C(Cp) chain of the chelating arm deviates from planarity but the ^{1}H NMR data clearly reveal for all the chelated complexes studied the occurrence of a fluxional process described essentially as an inversion of the Rh–P–CH_2–CH_2–C_5H_4 ring. In **14**, this process is faster than the internal rotation also observed for the ethylene ligand.

Introduction

As ancilliary heterodifunctional ligands, the cyclopentadienylphosphines[1] can be considered as combining the properties of their constituent moieties and therefore deserve much attention for monometallic as well as homo- or heterobimetallic complexes possibly efficient in transition-metal-catalyzed reactions. In contrast with the directly linked system C_5H_4–PPh_2, acting preferentially as a bridging ligand,[2] the derivatives in which an alkyl spacer is introduced between the cyclopentadienyl and phosphine fragments should allow chelate formation.[1a,3] Interesting phenomena, including mononuclear–binuclear–polymer interrelations, dissociation of the alkylphosphine side arm together with formation of vacant coordination sites, etc., call for further structural, thermodynamic, and kinetic studies.

• Abstract published in *Advance ACS Abstracts*, June 1, 1994.

(1) (a) Charrier, C.; Mathey, F. *J. Org. Chem.* **1979**, *170*, C41–C43. (b) Schore, N. E. *J. Am. Chem. Soc.* **1979**, *101*, 7410–7412. (c) Szymoniak, J.; Besançon, J.; Dormond, A.; Moise, C. *J. Org. Chem.* **1990**, *55*, 1429–1432. (d) Bensley, D. M.; Mintz, E. A., Jr. *J. Organomet. Chem.* **1988**, *353*, 93–102.

(2) (a) Leblanc, J.-C.; Moise, C.; Maisonnat, A.; Poilblanc, R.; Charrier, C.; Mathey, F. *J. Org. Chem.* **1982**, *231*, C43–C48. (b) Casey, C. P.; Bullock, R. M. *Organometallics* **1982**, *1*, 1591–1596. (c) Rausch, M. D.; Edwards, B. H.; Rogers, R. D.; Atwood, J. L. *J. Am. Chem. Soc.* **1983**, *105*, 3882–2886. (d) Casey, C. P.; Bullock, R. M.; Nief, F. *J. Am. Chem. Soc.* **1983**, *105*, 7574–7580. (e) Casey, C. P.; Nief, F. *Organometallics* **1985**, *4*, 1218–1220. (f) Tikkanen, W.; Fujita, Y.; Petersen, J. L. *Organometallics* **1986**, *5*, 888–894. (g) Bullock, R. M.; Casey, C. P. *Acc. Chem. Res.* **1987**, *20*, 167–173. (h) He, X. D.; Maisonnat, A.; Dahan, F.; Poilblanc, R. *Organometallics* **1987**, *6*, 678–680. (i) He, X. D.; Maisonnat, A.; Dahan, F.; Poilblanc, R. *Organometallics* **1989**, *8*, 2618–2626. (j) He, X. D.; Maisonnat, A.; Dahan, F.; Poilblanc, R. *Organometallics* **1991**, *10*, 2443–2456. (k) Brumas, B.; Dahan, F.; de Montauzon, D.; Poilblanc, R. *J. Organomet. Chem.* **1993**, *453*, C_{13}–C_{15}. (l) Brumas, B.; de Caro, D.; Dahan, F.; de Montauzon, D.; Poilblanc, R. *Organometallics* **1993**, *12*, 1503–1505.

(3) (a) Slawin, A. M. Z.; Williams, D. J.; Crosby, J.; Ramsden, J. A.; White, J. A. *J. Chem. Soc., Dalton Trans.* **1988**, 2491. (b) Kettenbach, R. T.; Butenschon, H. *New J. Chem.* **1990**, *14*, 599–601. (c) Butenschön, H.; Kettenbach, R. T.; Krüger, K. *Angew. Chem., Int. Ed. Engl.* **1992**, *31*, 1066–1067.

0276-7333/94/2313-2743$04.50/0

More specifically, syntheses and studies concerning the (cyclopentadienylethyl)diphenylphosphine ligand and its derivatives have been reported in the cases of manganese,[1a] ruthenium,[3a] and cobalt[3b,c] complexes, while various studies have used the related (cyclopentadienylethyl)-amine ligands in cobalt and iron,[4] molybdenum and tungsten,[5] and zirconium and hafnium[6] chemistry.

Herein we focus on the preparations of various rhodium(I) and iridium(I) complexes of (cyclopentadienylethyl)-diphenylphosphine. The first series of observations on their reactivity is also reported together with X-ray diffraction studies of two chelated complexes, with ethene ($(\eta^5{:}\eta^1\text{-}C_5H_4(CH_2)_2PPh_2)Rh^I(C_2H_4)$) and diiodo ligands ($(\eta^5{:}\eta^1\text{-}C_5H_4(CH_2)_2PPh_2)Rh^{III}I_2$).

Experimental Section

General Remarks. All reactions and manipulations were routinely performed under a nitrogen or argon atmosphere in Schlenk-type glassware. All solvents were appropriately purified before use by distillation from sodium/benzophenone or CaOH. Microanalyses were performed by the service de Microanalyses du laboratoire de Chimie de Coordination du CNRS. Mass spectra were recorded on a Varian MAT 311 A instrument. Infrared spectra in THF or dichloromethane solutions were recorded using a Perkin-Elmer Model 983 grating spectrometer. ^1H NMR spectra were obtained at 90 MHz on a Bruker WH 90 FT, at 200.13 MHz on a Bruker AC 200 FT, or at 250.1 MHz on a Bruker WM 250 FT spectrometer. ^{31}P NMR spectra were recorded at 32.4 MHz on a Bruker WH 80 FT spectrometer, and chemical shifts were referenced to external H_3PO_4. ^{13}C NMR spectra were obtained at 50.3 MHz.

Preparation of Compounds. [((Diphenylphosphino)ethyl)-cyclopentadienyl]lithium (1) was prepared by $LiPPh_2$ addition to spiro[2.4]hepta-4,6-diene, following the published procedure.[7] The starting materials $[RhCl(CO)_2]_2$[8a] (2), $[IrCl(coe)_2]_2$[8b] (coe = 1,5-cyclooctene) (3), $[IrCl(cod)]_2$[8c] (cod = 1,5-cyclooctadiene) (4), RhCl(cod)[8d] (5), $[RhCl(C_2H_4)_2]_2$[8e] (6), and Vaska's complex[8f] (7) were also prepared according to well-known procedures.

$(\eta^5{:}\eta^1\text{-}C_5H_4(CH_2)_2PPh_2)Rh(CO)$ (8). A solution of $[RhCl(CO)_2]_2$ (2; 80 mg, 0.2 mmol) in 10 mL of THF was treated by dropwise addition of a solution of $Cp(CH_2)_2PPh_2Li$ (0.4 mmol) in 10 mL of THF. The solution was warmed to 50 °C and stirred for 7 h. The solvent was removed in vacuo, and the residue was eluted through an alumina column with toluene and pentane (4:1). The resulting yellow solution was pumped to dryness (yellow powder); yield 70%. Mass spectrometry: m/e 408 (M^+), 380 ($M^+ - CO$). Anal. Calcd for $C_{20}H_{18}RhPO$: C, 58.85; H, 4.44. Found: C, 58.84; H, 4.38.

Formation and Identification in Solution of $[(\mu\text{-}\eta^5{:}\eta^1\text{-}C_5H_4(CH_2)_2PPh_2)Rh(CO)]_2$ (9a,b). A solution of $[RhCl(CO)_2]_2$ (50 mg, 0.2 mmol) in 10 mL of THF was treated dropwise with a solution of $Cp(CH_2)_2PPh_2Li$ (0.4 mmol) in 10 mL of THF. The solution was stirred for 7 h. The solvent was removed in vacuo, and the brown residue was eluted by toluene. The solution was evaporated. The resulting solid was a mixture containing $(\eta^5{:}\eta^1\text{-}C_5H_4(CH_2)_2PPh)Rh(CO)$ (8) and $[(\mu\text{-}\eta^5{:}\eta^1\text{-}C_5H_4(CH_2)_2PPh_2)Rh(CO)]_2$ (9a,b). Mass spectrometry (DCI/NH_3): 8, m/e 409 ($M^+ + 1$); 9a,b, m/e 789 ($M^+ - 28 + 1$).

$(\eta^5{:}\eta^1\text{-}C_5H_4(CH_2)_2PPh_2)Ir^I(CO)$ (10). A slurry of $IrCl(CO)(PPh_3)_2$ (117 mg, 0.15 mmol) in 10 mL of THF was treated dropwise with a solution of $Cp(CH_2)_2PPh_2Li$ (0.3 mmol) in 10 mL of THF. The solution was stirred for 15 h, and the solvent was removed in vacuo. The residue was eluted with toluene, affording a mixture of 10 and PPh_3. Mass spectrometry (DCI/NH_3): m/e 499 ($M^+ + 1$).

$(\eta^5{:}\eta^1\text{-}C_5H_4(CH_2)_2PPh_2)Ir(C_2H_4)$ (12). The compound $[IrCl(coe)_2]_2$ (3; 90 mg, 0.1 mmol) was added to 20 mL of diethyl ether in a 50-mL Schlenk flask. Ethylene was passed through the orange slurry at 0 °C for 0.5. This resulted in a colorless solution of $[Ir^ICl(C_2H_4)]_n$. To this solution was added a solution of $Cp(CH_2)_2PPh_2Li$ (0.3 mmol) in 10 mL of THF. After the mixture was stirred for 15 h, LiCl had precipitated and the yellow solution was filtered. The filtered solution was pumped to dryness and the residue washed with diethyl ether (2 × 1 mL); yield 60%. The analytical data were never entirely satisfactory; therefore, the product was further identified from its quantitative reaction with iodine leading to 17.

$(\eta^5{:}\eta^1\text{-}C_5H_4(CH_2)_2PPh_2)Rh(C_2H_4)$ (14). A solution of $[RhCl(C_2H_4)_2]_2$ (6; 80 mg, 0.2 mmol) in 10 mL of diethyl ether was treated with $Cp(CH_2)_2PPh_2Li$ (0.4 mmol) in 10 mL of THF. The reaction mixture was stirred for 15 h, leading to a brown solution which was pumped to dryness. Then the residue, dissolved in a pentane–toluene mixture (1:1), was eluted through an alumina column. The resulting product was recrystallized from a saturated pentane solution at room temperature, leading to orange-yellow crystals. Anal. Calcd for $C_{21}H_{22}RhP$: C, 61.78; H, 5.43. Found: C, 61.61; H, 5.40.

$(\eta^5\text{-}C_5H_4(CH_2)_2PPh_2)Rh(cod)$ (15). $[RhCl(cod)]_2$ (98.6 mg, 0.2 mmol) was dissolved in 10 mL of THF. A solution of $Cp(CH_2)_2PPh_2Li$ (0.4 mmol) in 10 mL of THF then was added. After it was stirred for 20 h, the resulting brown solution was filtered and pumped to dryness. The residue was eluted with a mixture of toluene and pentane (4:1) and filtered. The solvent was removed under vacuum.

$(\eta^5\text{-}C_5H_4(CH_2)_2PPh_2)Ir(cod)$ (16). $[IrCl(cod)]_2$ (135 mg, 0.2 mmol) was dissolved in 10 mL of THF. The solution was degassed with one freeze–pump–thaw cycle. A solution of $Cp(CH_2)_2PPh_2Li$ (0.4 mmol) in 10 mL of THF then was added. After it was stirred for 20 h, the yellow solution was filtered and pumped to dryness. The residue was soluble in toluene, and this solution was filtered through a small pad of alumina. The solvent then was removed under vacuum. The resulting solid was washed with pentane. Mass spectrometry (EI): m/e 578.

$(\eta^5{:}\eta^1\text{-}C_5H_4(CH_2)_2PPh_2)RhI_2$ (17). A solution of iodine (30 mg, 0.12 mmol) in 20 mL of CH_2Cl_2 was added to a yellow solution of 40.8 mg (0.1 mmol) of $(\eta^5\text{-}C_5H_4(CH_2)_2PPh_2)Rh^I(CO)$ (8). The resulting solution was stirred for 30 min, turning to red-brown, and the solvent was removed to dryness. The residue was recrystallized from CH_2Cl_2/diethyl ether (1:5) to give red-brown crystals. Anal. Calcd for $C_{19}H_{18}PRhI_2$ (mol wt 636.2): C, 35.87; H, 2.85. Found: C, 35.85; H, 3.05.

$(\eta^5{:}\eta^1\text{-}C_5H_4(CH_2)_2PPh_2)IrI_2$ (18). A solution of iodine (30 mg, 0.12 mmol) in 20 mL of CH_2Cl_2 was added to a solution of $(\eta^5{:}\eta^1\text{-}C_5H_4(CH_2)_2PPh_2)Ir^I(C_2H_4)$ (12; 50 mg, 0.1 mmol) in 5 mL of CH_2Cl_2. The mixture was stirred for 1 h, affording a red-brown solution. This solution was pumped to dryness and the residue recrystallized from CH_2Cl_2/diethyl ether. Anal. Calcd for $C_{19}H_{18}PIrI_2$: C, 31.55; H, 2.51. Found: C, 31.73; H, 2.70.

X-ray Crystallography. Crystal data for $(\eta^5{:}\eta^1\text{-}C_5H_4(CH_2)_2PPh_2)Rh(C_2H_4)$ (14) and $(\eta^5{:}\eta^1\text{-}C_5H_4(CH_2)_2PPh_2)RhI_2$ (17) are summarized in Table 1.

Structure Determination. Reflection data were measured at 20 °C with an Enraf-Nonius CAD-4 diffractometer in the $\omega/2\theta$ scan mode using graphite-monochromatized Mo Kα radiation (λ = 0.710 73 Å). A least-squares fit of 25 reflections was used to obtain the final lattice parameters and the orientation matrix.

(4) (a) Jutzi, P.; Kristen, M. O.; Dahlhaus, J.; Neumann, B.; Stammler, H. G. *Organometallics* **1993**, *12*, 2980–2985. (b) Jutzi, P.; Dahlhaus, J.; Kristen, M. O. *J. Organomet. Chem.* **1993**, *450*, C1–C3.

(5) (a) Wang, T. F.; Lee, T. Y.; Wen, Y. S.; Liu, L.-W. *J. Organomet. Chem.* **1991**, *403*, 353–358. (b) Wang, T. F.; Lee, T. Y.; Chou, J. W.; Ong, C. W. *J. Organomet. Chem.* **1992**, *423*, 31–38. (c) Wang, T. F.; Wen, Y. S. *J. Organomet. Chem.* **1992**, *439*, 155–162. (d) Avey, A.; Weakley, J. R.; Tyler, D. R. *J. Am. Chem. Soc.* **1993**, *115*, 7706–7715.

(6) Hughes, A. K.; Meetsma, A.; Teuben, J. H. *Organometallics* **1993**, *12*, 1936–1945.

(7) Kauffman, T.; Bisling, M.; König, R.; Rensing, A.; Steinseifer, F.; Wolterman, A. *Angew. Chem., Int. Ed. Engl.* **1980**, *19*, 328–329.

(8) (a) Gallay, J.; de Montauzon, D.; Poilblanc, R. *J. Organomet. Chem.* **1972**, *38*, 179–197 and references therein. (b) Van der Ent, A.; Onderdelinden, A. L. *Inorg. Synth.* **1973**, *14*, 92. (c) Winkhaus, G.; Singer, H. *Chem. Ber.* **1966**, *99*, 3610. (d) Chatt, J.; Venanzi, L. M. *J. Chem. Soc.* **1957**, 4735. (e) Cramer, R. *J. Am. Chem. Soc.* **1964**, *86*, 217. (f) Burk, M. J.; Crabtree, R. H. *Inorg. Chem.* **1986**, *25*, 931–932.

Table 1. Crystal Data for $(\eta^5:\eta^1\text{-}C_5H_4(CH_2)_2PPh_2)Rh(C_2H_4)$ (14) and $(\eta^5:\eta^1\text{-}C_5H_4(CH_2)_2PPh_2)RhI_2$ (17)

	14	17
formula	$C_{21}H_{22}PRh$	$C_{19}H_{18}I_2PRh$
fw	408.3	634.0
cryst syst	monoclinic	monoclinic
space group	$P2_1/n$	$P2_1/n$
a, Å	9.808(1)	10.439(1)
b, Å	28.515(3)	16.557(2)
c, Å	13.094(1)	11.458(1)
β, deg	98.34(1)	95.85(1)
V, Å^3	3623.3(8)	1970.1(8)
Z	8	4
$F(000)$	1664	1192
D_c, g cm^{-3}	1.497	2.138
λ, Å	0.710 73	0.710 73
μ(Mo Kα), cm^{-1}	9.5	40.35
transmissn coeff (min–max)	0.963–0.999	0.891–1.000
$2\theta_{max}$, deg	46	44
no. of rflns measd	5033 total, 5033 unique	2407 total, 2407 unique
observn criterion	$F_o^2 > 3\sigma(F_o^2)$	$F_o^2 > 3\sigma(F_o^2)$
no. of obsd rflns	3035	1638
$R(F_o)$	0.031	0.027
R_w	0.038	0.039

Data were reduced in the usual way with the MolEN package.[9] There was no significant variation of standards. An empirical absorption correction[10] was applied on the basis of ψ scans.

$(\eta^5:\eta^1\text{-}C_5H_4(CH_2)_2PPh_2)Rh(C_2H_4)$ (14). Orange-yellow plates were obtained at room temperature by slow evaporation from a saturated pentane solution. The structure was determined by direct methods, using the SHELXS-86 program.[11a] Refinements were carried out with the SHELX-76 program[11b] using full-matrix least-squares techniques minimizing the function $\sum w(|Fo|-|Fc|)^2$. Phenyl rings were refined as isotropic rigid groups (C–C = 1.395 Å). All other non-H atoms were refined anisotropically. All H atoms were observed but introduced in calculations in idealized geometry (C–H = 0.97 Å), but those of C_2H_4 were allowed to vary. Their temperature factors were first allowed to vary and then kept fixed to 0.055 Å^2. Atomic scattering factors (f', f'') were taken from the literature.[12] The refinement converged to R = 0.031 and R_w = 0.038 with a maximum shift/esd of 0.030 on the final cycle with 3035 observations and 271 variable parameters. A fit of S = 1.03 for the data using the weighting scheme $w = [\sigma^2(F_o) + 0.0005F_o^2]^{-1}$ was obtained. The maximum residual peak was 0.5 e/Å^3 near the Rh atoms. Table 2 lists the atomic positions for the non-hydrogen atoms. An ORTEP diagram[13] of 14 is shown in Figure 2.

$(\eta^5:\eta^1\text{-}C_5H_4(CH_2)_2PPh_2)RhI_2$ (17). Dark red plates were obtained by slow diffusion of pentane into a dichloromethane solution. The structure of 17 was solved by the Patterson method, using the SHELXS-86 program.[11a] All other atoms were found by difference-Fourier-map calculations. Phenyl rings were refined as isotropic rigid groups (C–C = 1.395 Å) as for 14. All other non-H atoms were refined anisotropically. All H atoms were observed and introduced in idealized geometry (C–H = 0.97 Å), with two general isotropic temperature factors that were first allowed to vary and then kept fixed to 0.05 Å^2 for methylene H atoms and to 0.06 Å^2 for the other H atoms. Atomic scattering factors (f', f'') are taken from ref 12 as for 14. The refinement converged to R = 0.027 and R_w = 0.039 with a maximum shift/esd of 0.020 on the final cycle with 1638 observations and 124 variable parameters. A fit of S = 1.35 for the data using the weighting scheme $w = [\sigma^2(F_o) + 0.0005F_o^2]^{-1}$ was obtained. The maximum residual peak was 0.8 e/Å^3 on I atoms. Table 3 gives the atomic positions for the non-hydrogen atoms. An ORTEP diagram[13] of 17 is shown in Figure 3.

Table 2. Fractional Atomic Coordinates and Isotropic or Equivalent Isotropic Temperature Factors (Å^2 × 100) for 14

atom	x	y	z	U_{eq}[a]/U_{iso}[a]
Rh(a)	0.36739(4)	0.65810(2)	0.53388(3)	3.49(3)
P(a)	0.5134(1)	0.69777(5)	0.6434(1)	3.5(1)
C(1a)	0.4892(6)	0.7584(2)	0.5951(4)	5.0(5)
C(2a)	0.4750(6)	0.7558(2)	0.4778(4)	5.6(5)
C(3a)	0.3735(6)	0.7179(2)	0.4359(4)	4.8(5)
C(4a)	0.3994(6)	0.6790(2)	0.3738(4)	4.7(5)
C(5a)	0.2810(6)	0.6505(3)	0.3627(4)	6.2(5)
C(6a)	0.1798(6)	0.6726(3)	0.4113(4)	6.1(5)
C(7a)	0.2344(6)	0.7151(2)	0.4538(4)	5.5(5)
C(8a)	0.4146(6)	0.5909(2)	0.5949(5)	5.8(5)
C(9a)	0.3031(6)	0.6091(2)	0.6382(4)	5.5(5)
C(10a)	0.4955(4)	0.6997(1)	0.7798(3)	3.8(2)*
C(11a)	0.5604(4)	0.6651(1)	0.8447(3)	5.2(2)*
C(12a)	0.5396(4)	0.6631(1)	0.9478(3)	6.1(2)*
C(13a)	0.4539(4)	0.6958(1)	0.9860(3)	5.6(2)*
C(14a)	0.3890(4)	0.7304(1)	0.9211(3)	6.2(2)*
C(15a)	0.4098(4)	0.7324(1)	0.8180(3)	5.1(2)*
C(16a)	0.6986(4)	0.6887(1)	0.6460(3)	3.3(2)*
C(17a)	0.7924(4)	0.7195(1)	0.7010(3)	4.5(2)*
C(18a)	0.9332(4)	0.7143(1)	0.6979(3)	5.3(2)*
C(19a)	0.9801(4)	0.6783(1)	0.6398(3)	5.3(2)*
C(20a)	0.8862(4)	0.6475(1)	0.5849(3)	6.0(2)*
C(21a)	0.7455(4)	0.6526(1)	0.5879(3)	4.5(2)*
Rh(b)	0.69855(5)	0.58320(2)	0.21826(4)	3.31(3)
P(b)	0.8758(1)	0.55378(6)	0.1561(1)	3.5(1)
C(1b)	0.8021(5)	0.4999(2)	0.0902(4)	4.4(4)
C(2b)	0.7094(6)	0.4775(2)	0.1591(4)	4.8(4)
C(3b)	0.6163(5)	0.5132(2)	0.1978(4)	4.3(4)
C(4b)	0.6125(6)	0.5243(2)	0.3044(4)	5.2(5)
C(5b)	0.5249(6)	0.5627(2)	0.3086(5)	5.5(5)
C(6b)	0.4653(5)	0.5743(2)	0.2050(5)	5.4(5)
C(7b)	0.5182(5)	0.5434(2)	0.1378(5)	5.3(5)
C(8b)	0.8005(6)	0.6425(2)	0.2894(5)	6.2(6)
C(9b)	0.7346(6)	0.6547(2)	0.1931(5)	5.9(5)
C(10b)	0.9602(3)	0.5848(2)	0.0597(3)	3.7(2)
C(11b)	0.8871(3)	0.5905(2)	–0.0391(3)	4.5(2)*
C(12b)	0.9484(3)	0.6131(2)	–0.1153(3)	5.7(2)*
C(13b)	1.0828(3)	0.6301(2)	–0.0926(3)	5.6(2)*
C(14b)	1.1559(3)	0.6244(2)	0.0062(3)	6.2(2)*
C(15b)	1.0946(3)	0.6018(2)	0.0824(3)	5.4(2)*
C(16b)	1.0210(4)	0.5311(2)	0.2468(3)	3.9(2)*
C(17b)	1.0219(4)	0.5377(2)	0.3525(3)	4.9(2)*
C(18b)	1.1283(4)	0.5190(2)	0.4229(3)	6.2(2)*
C(19b)	1.2339(4)	0.4936(2)	0.3876(3)	6.6(2)*
C(20b)	1.2330(4)	0.4870(2)	0.2819(3)	6.0(2)*
C(21b)	1.1265(4)	0.5058(2)	0.2115(3)	5.2(2)*

[a] $U_{eq} = {}^1/_3(U_{11} + U_{22} + U_{33})$. Asterisks denote isotropic U values.

Results and Discussion

Modes of Reactivity and Chelating and Bridging Properties of (Cyclopentadienylethyl)diphenylphosphine toward the Rhodium and Iridium Carbonyl Derivatives. The first aim of our research was to explore the potential of (cyclopentadienylethyl)diphenylphosphine with regard to the tailoring of new structures in rhodium and iridium chemistry.

By an approach similar to that used with the parent ligand cyclopentadienylphosphine,[2h–j] the reaction with chlorodicarbonylrhodium(I) was performed, by adding a THF solution of [((diphenylphosphino)ethyl)cyclopentadienyl]lithium to a THF solution of 1. Monitoring the reaction by ^{31}P NMR spectroscopy at 32 MHz at room temperature showed that after 12 h the starting material

(9) Fair, C. K. MolEN: Structure Solution Procedures; Enraf-Nonius: Delft, Holland, 1990.
(10) North, A. C. T.; Phillips, D. C.; Mathews, F. S. *Acta Crystallogr., Sect. A* **1968**, *A21*, 351–359.
(11) (a) Sheldrick, G. M. SHELXS-86: Program for Crystal Structure Solution; University of Gottingen: Gottingen, Federal Republic of Germany, 1986. (b) Sheldrick, G. M. SHELX 76: Program for Crystal Structure Determination; University of Cambridge: Cambridge, England, 1976.
(12) *International Tables for X-Ray Crystallography*; Kynoch Press: Birmingham, England, 1974; Vol. IV, Table 2.2.B, pp 99–101.
(13) Johnson, C. K. ORTEP; Report ORNL-3794; Oak Ridge National Laboratory: Oak Ridge, TN, 1965.

Table 3. Fractional Atomic Coordinates and Isotropic or Equivalent Isotropic Temperature Factors (Å² × 100) for 17

atom	*x*	*y*	*z*	U_{eq}/U_{iso}
I(1)	0.67914(7)	0.17098(5)	0.35548(7)	9.26(6)
I(2)	0.31382(7)	0.12465(4)	0.32219(6)	7.29(5)
Rh	0.48707(5)	0.18094(3)	0.48981(5)	3.71(4)
P	0.4481(2)	0.3134(1)	0.4502(2)	3.7(1)
C(1)	0.5193(7)	0.3584(5)	0.5898(7)	4.8(5)
C(2)	0.4703(8)	0.3096(5)	0.6873(7)	5.1(5)
C(3)	0.4913(8)	0.2223(5)	0.6674(6)	4.8(5)
C(4)	0.3971(8)	0.1602(5)	0.6515(7)	5.5(5)
C(5)	0.4582(8)	0.0856(5)	0.6248(7)	5.4(5)
C(6)	0.5891(9)	0.1010(5)	0.6251(8)	6.1(6)
C(7)	0.6116(8)	0.1847(5)	0.6483(7)	5.3(5)
C(8)	0.5149(5)	0.3663(3)	0.3324(4)	3.8(2)*
C(9)	0.6058(5)	0.4275(3)	0.3551(4)	5.4(2)*
C(10)	0.6506(5)	0.4702(3)	0.2624(4)	6.3(2)*
C(11)	0.6044(5)	0.4516(3)	0.1470(4)	6.8(3)*
C(12)	0.5134(5)	0.3904(3)	0.1242(4)	6.9(3)*
C(13)	0.4687(5)	0.3477(3)	0.2169(4)	5.8(2)*
C(14)	0.2809(4)	0.3469(2)	0.4400(5)	3.4(2)*
C(15)	0.2490(4)	0.4250(2)	0.4019(5)	4.3(2)*
C(16)	0.1224(4)	0.4523(2)	0.4004(5)	5.1(2)*
C(17)	0.0277(4)	0.4014(2)	0.4370(5)	5.1(2)*
C(18)	0.0597(4)	0.3233(2)	0.4751(5)	6.2(2)*
C(19)	0.1863(4)	0.2960(2)	0.4766(5)	4.8(2)*

[a] $U_{eq} = {}^1/_3(U_{11} + U_{22} + U_{33})$. Asterisks denote isotropic *U* values.

was completely consumed. Three major types of products were formed, characterized by doublets at ca. 25 ppm with doublet spacings of about 125 Hz (compound $\mathbf{i}_1$, δ 23.01 ppm, J_{P-Rh} = 124.5 Hz; compound $\mathbf{i}_2$, δ 23.67 ppm, J_{P-Rh} = 125.1 Hz), around 45 ppm with doublet spacings around 200 Hz (**9a**, δ 43 ppm, J_{P-Rh} = 196 Hz; **9b**, δ 45.15 ppm, J_{P-Rh} = 196 Hz) and at δ 73.95 ppm (J_{P-Rh} = 204.4 Hz, **8**).

Compound **8** was characterized by ^{31}P and ^1H NMR (Tables 4 and 5), infrared spectroscopy, mass spectroscopy, and elemental analysis to be the rhodium(I) mononuclear d^8 chelated compound (η^5:η^1-$C_5H_4(CH_2)_2PPh_2$)Rh(CO).

The formation of the labile compounds **9a,b** appeared to be favored during the early period of the experiment at room temperature. When the temperature of the reaction mixture was increased or the reaction was carried out for a longer period of time, **9a,b** disappeared, leading to the formation of **8** only. In a typical experiment at room temperature, the ratio **9a,b**/**8** decreased, from 20 at the beginning of the reaction to zero after 5 h. The mixture of **8** and **9a,b** was identified by mass spectrometry as containing monomeric and dimeric species (mass spectrometry (DCI/NH_3): **8**, *m/e* 409 (M^+ + 1); **9a,b**, *m/e* 789 (M^+ - 28 + 1)).

The compounds $\mathbf{i}_1$ and $\mathbf{i}_2$ were identified as the primary intermediates occurring from **2**, by the nucleophilic attack of **1** acting as a phosphine. Indeed, as in our previous studies concerning the reaction of ((diphenylphosphino)-cyclopentadienyl)thallium with the chloro-bridged carbonyl species **2**,[2h] the bonding of the phosphorus atom to a rhodium(I) center was easily distinguished by considering the value of the coupling constant J_{P-Rh}. The observed values are very close to those measured in a series of 16-electron square-planar mononuclear (η^1-$TlC_5H_4Ph_2P$)-$RhCl(CO)_2$ (J_{P-Rh} = 121.3 Hz) and dinuclear *cis*- and *trans*-[(η^1-$TlC_5H_4Ph_2P$)$Rh(\mu$-Cl)(CO)]$_2$ (J_{P-Rh} = 117.6 and 119.8 Hz) complexes. Similarly, in the bimetallic compound $RhCl(CO)(PPh_3)[[\mu$-η^1-$Ph_2P(\eta^5$-$C_5H_4)]Rh(CO)_2]$, the cyclopentadienyldiphenylphosphine ligand bonded through the phosphorus atom to the 16-electron rhodium center is characterized by a value for the J_{P-Rh} constant (123.5 Hz) of the same magnitude. If a square-planar coordination is assigned to the rhodium atom in the intermediates $\mathbf{i}_1$ and $\mathbf{i}_2$, two possibilities are still offered, leading us to consider them *a priori* either as mononuclear or as dinuclear species (*vide infra*).

Interestingly, the IR spectra of solutions containing the three compounds **8** and **9a,b** show apparently a single but large C–O stretching band (at 1934 cm^{-1} in THF or CH_2Cl_2) (Table 4) whose intensity was practically unchanged when—as observed by NMR—the ratio of the concentrations [**8**]/[**9a**]/][)9b] varied. These observations are in agreement with almost equal values of the C–O stretching frequencies for the three compounds. Indeed, in the dinuclear isomers **9a,b** (Figure 1) the interactions between the two C–O vibrators are expected to be almost absent, leading therefore to the existence of only one mode of vibration instead of a pair of symmetric and antisymmetric modes. In addition, similar local structures around the central atoms in the three compounds **8** and **9a,b** imply equal values for their C–O frequencies. In agreement with all these spectroscopic data, the Figure 1 identifies **9a,b** as the two expected *cisoid* and *transoid* isomers of the ((diphenylphosphino)ethyl)cyclopentadienyl-bridged dinuclear compound [(μ-η^5:η^1-$C_5H_5(CH_2)_2PPh_2$)$Rh(CO)]_2$.[14]

Figure 1 is an attempt to rationalize the general synthetic pathways from compound **1** to compound **8**. Owing to the large predominance of the dinuclear species **9a,b** in the early stage of the reaction, it is assumed that these compounds are the kinetic products, transforming slowly into the thermodynamically more stable chelated monomer **8**. In such a case, the absence of **8** at the very beginning of the reaction also favors the proposal that **9a,b** are formed during the early stage of the reaction. In our opinion only an intramolecular process from dinuclear species could explain the transient formation of the kinetic products **9a,b** instead of the direct formation of the stable chelated monomer **8**. This leads us therefore to consider $\mathbf{i}_1$ and $\mathbf{i}_2$ as the doubly square planar species[15] shown in Figure 1.

In order to extend the preceeding results to iridium chemistry, we have used Vaska's complex (**7**) as starting material. The reaction performed in THF solution appeared to be slower than the overall process observed with rhodium materials. In such a process, the first step consists of the substitution of one of the triphenylphosphine ligands of **7**—as shown by the occurrence of its characteristic peak in the ^{31}P NMR spectrum—by the phosphine end of **1**. The expected planar intermediate (η^1-$C_5H_4(CH_2)_2PPh_2$)$IrCl(CO)(PPh_3)$ (**i**) was identified by infrared spectroscopy in the C–O stretching absorption range at 1954 cm^{-1} during the early period of the reaction. Indeed as expected, this band disappeared when the reaction progressed, leading to the appearance of a new band at 1916 cm^{-1}, while the ^{31}P NMR spectrum consists of singlets. From these resonances, only the major species

(14) From the manipulation of compact molecular models, the occurrence of these *cisoid* and *transoid* conformations seems perfectly acceptable, but in contrast with the case of $CpPPh_2$ derivatives,[16] a larger flexibility of the structures could be expected. Other conformations of low energy seem possible and could explain other minor $\delta(^{31}P)$ signals of very low intensities observed around 40 ppm.

(15) Further experiments starting from the complexes [RhCl(CO)-$(C_2H_4)]_2$ and [Rh(SPh)$(CO)_2]_2$, well-known as affording dinuclear phosphine-substituted derivatives,[16] do not lead to more stable intermediates analogous to $\mathbf{i}_1$ and $\mathbf{i}_2$ and therefore do not offer models for the proposed pathway from the staring materials **2–8**.

(16) (a) Maisonnat, A.; Kalck, P.; Poilblanc, R. *Inorg. Chem.* **1974**, *13*, 2996–3001. (b) Bonnet, J.-J.; Kalck, P.; Poilblanc, R. *Inorg. Chem.* **1977**, *16*, 1514–1518.

(17) Hoffman, P.; Heiss, H.; Muller, G. *Z. Naturforsch.* **1987**, *B42*, 395–401.

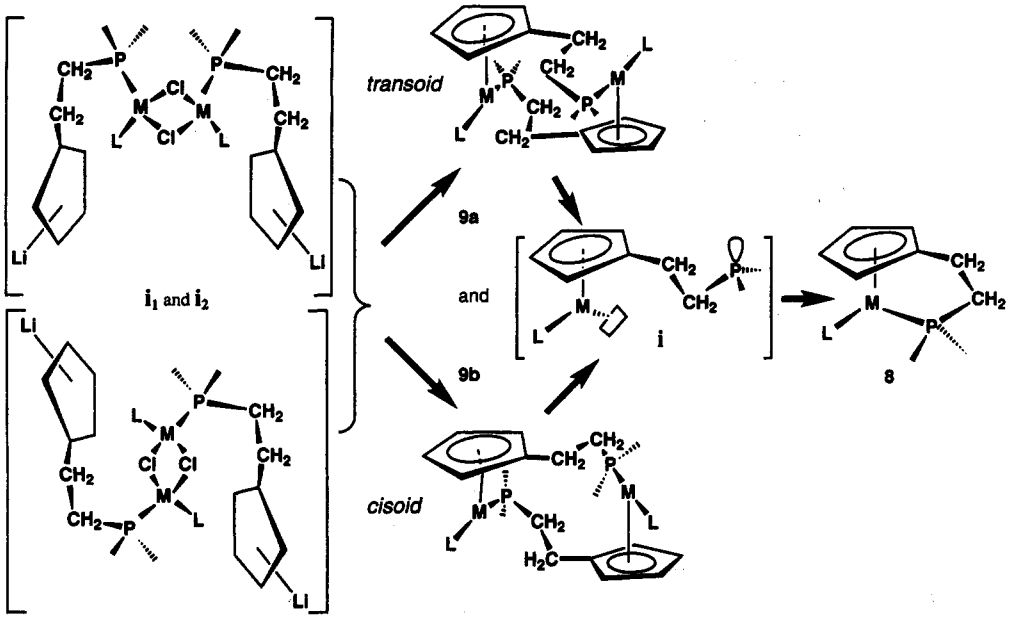

Figure 1. Proposed pathways to $(\eta^5{:}\eta^1\text{-}C_5H_4(CH_2)_2PPh_2)Rh(CO)$ (8) from the $[RhCl(CO)_2]_2/C_5H_4(CH_2)_2PPh_2Li$ system in THF.

Table 4. $^{31}P\{^1H\}$ NMR Data and C–O Stretching Frequencies of the ((Cyclopentadienylethyl)diphenylphosphine)rhodium and -iridium Complexes

	$\delta(^{31}P)$, ppm (in C_6D_6)	$^1J_{PRh}$, Hz	$\nu(CO)$, cm^{-1} (in THF)
$(\eta^5{:}\eta^1\text{-}C_5H_4(CH_2)_2PPh_2)Rh(CO)$ (**8**)	73.65 d	204.4	1934 (1947 in hexane)
$[(\mu\text{-}\eta^5{:}\eta^1\text{-}C_5H_4(CH_2)_2PPh_2)Rh(CO)]_2$ (**9a**)	43.68 d	195.2	1934
$[(\mu\text{-}\eta^5{:}\eta^1\text{-}C_5H_4(CH_2)_2PPh_2)Rh(CO)]_2$ (**9b**)	44.11 d	194.6	1934
$[(\eta^1\text{-}LiC_5H_4(CH_2)_2PPh_2)Rh(CO)_2Cl]_n$ (i_1)	23.01 d	124.5	1969
$[(\eta^1\text{-}LiC_5H_4(CH_2)_2PPh_2)Rh(CO)_2Cl]_n$ (i_2)	23.67 d	125.1	1969
$(\eta^5{:}\eta^1\text{-}C_5H_4(CH_2)_2PPh_2)Ir(CO)$ (**10**)	34.64 s		1916
$[(\mu\text{-}\eta^5{:}\eta^1\text{-}C_5H_4(CH_2)_2PPh_2)Ir(CO)]_2$ (**11**)	7.66 s		1916
$(\eta^5{:}\eta^1\text{-}C_5H_4(CH_2)_2PPh_2)Ir(C_2H_4)$ (**12**)	26.97 s		
$(\eta^5{:}\eta^1\text{-}C_5H_4(CH_2)_2PPh_2)Ir(C_8H_{14})$ (**13**)	26.96 s		
$(\eta^5{:}\eta^1\text{-}C_5H_4(CH_2)_2PPh_2)Rh(C_2H_4)$ (**14**)	69.39 d	213.6	
$(\eta^5\text{-}C_5H_4(CH_2)_2PPh_2)Rh(C_8H_{12})$ (**15**)	−16.66 s		
$(\eta^5\text{-}C_5H_4(CH_2)_2PPh_2)Ir(C_8H_{12})$ (**16**)	−16.14 s		
$(\eta^5{:}\eta^1\text{-}C_5H_4(CH_2)_2PPh_2)RhI_2$ (**17**)	54.58 d	146.7	
$(\eta^5{:}\eta^1\text{-}C_5H_4(CH_2)_2PPh_2)IrI_2$ (**18**)	15.52 s		

Table 5. ^1H NMR Data for the Most Stable ((Cyclopentadienylethyl)diphenylphosphine)rhodium and -iridium Complexes

	δ_{H_a}, ppm	δ_{H_b}, ppm	δ_{H_c}, ppm	$^3J_{H_cP}$, Hz	$^3JH_cH_d$, Hz	δ_{H_d}, ppm	^2JH_dP, Hz
$(\eta^5{:}\eta^1\text{-}C_5H_4(CH_2)_2PPh_2)Rh(CO)$ (**8**)[a]	5.63 (m)	5.46 (m)	2.79 (dt)	9.3	6.9	1.84 (dt)	32.4
$(\eta^5{:}\eta^1\text{-}C_5H_4(CH_2)_2PPh_2)Ir(CO)$ (**10**)[a]	5.46 (m)	5.38 (m)	2.83 (dt)	9.8	6.7	1.70 (dt)	29.6
$(\eta^5{:}\eta^1\text{-}C_5H_4(CH_2)_2PPh_2)Ir(C_2H_4)$ (**12**)[a]	5.53 (m)	5.12 (m)	2.91 (dt)	9.5	6.9	1.77 (dt)	27.5
$(\eta^5{:}\eta^1\text{-}C_5H_4(CH_2)_2PPh_2)Ir(C_8H_{14})$ (**13**)[a]	5.57 (m)	5.07	3.34 (dt)	9.6	6.9	2.04 (dt)	27.6
$(\eta^5{:}\eta^1\text{-}C_5H_4(CH_2)_2PPh_2)Rh(C_2H_4)$ (**14**)[a]	5.87 (m)	5.30 (m)	2.87 (dt)	9.5	6.8	2.04 (dt)	30.7
$(\eta^5\text{-}C_5H_4(CH_2)_2PPh_2)Rh(C_8H_{12})$ (**15**)[a]	5.03 (m)	4.93 (m)					
$(\eta^5\text{-}C_5H_4(CH_2)_2PPh_2)Ir(C_8H_{12})$ (**16**)[a]	4.90 (m)	4.95 (m)					
$(\eta^5{:}\eta^1\text{-}C_5H_4(CH_2)_2PPh_2)RhI_2$ (**17**)[b]	5.35 (m)	4.85 (m)	2.66 (dt)	10.2	6.6	1.17 (dt)	32.7
$(\eta^5{:}\eta^1\text{-}C_5H_4(CH_2)_2PPh_2)IrI_2$ (**18**)[b]	6.04 (m)	5.57 (m)	3.10 (dt)	9.8	6.9	2.11 (dt)	28.1

[a] In C_6D_6. [b] In $CHCl_3$.

(δ 34.6 ppm) was identified by mass spectrometry as the mononuclear compound **10**, analogous to **8**. Unfortunately, the overall yield of the reaction is too low to be very useful for preparative purposes.

Extension to Iridium and Rhodium Olefin Derivatives. For the purpose of providing a better route to chelated iridium compounds, this study was extended to $[IrCl(C_2H_4)_2]_2$ (**3**) and $[IrCl(coe)]_2$ (**4**; coe = cyclooctene) as starting materials. In both cases, the reactions were performed at room temperature in THF solution and monitored by ^{31}P NMR spectroscopy. A series of compounds analogous to the preceding carbonyl compounds were detected and tentatively identified respectively as the primary phosphorus-bonded intermediate $(\eta^5{:}\eta^1\text{-}C_5H_4(CH_2)_2PPh_2)IrL_2$, as the kinetic dinuclear products $[(\mu\text{-}\eta^5{:}\eta^1\text{-}C_5H_4(CH_2)_2PPh_2)IrL]_2$ (for example **11** in Table 4), and and as the chelated mononuclear compound $(\eta^5{:}\eta^1\text{-}C_5H_4(CH_2)_2PPh_2)IrL$ (L = C_2H_4 (**12**), coe (**13**)) (Tables 4 and 5). In this series, our interest focused on compound **12**, which was prepared by reaction at 20 °C and then crystallized in diethyl ether as a rather unstable yellow powder. Compound **12** was identified by ^{31}P and ^1H NMR, but it gave poor elemental analysis.

With Cramer's dinuclear rhodium compound $[RhCl(C_2H_4)]_2$ (**6**) as starting material, the same types of reactions were performed, affording at room temperature in diethyl ether solution the monomeric compound $(\eta^5{:}\eta^1\text{-}C_5H_4(CH_2)_2PPh_2)Rh(C_2H_4)$ (**14**). This complex, obtained as a yellow

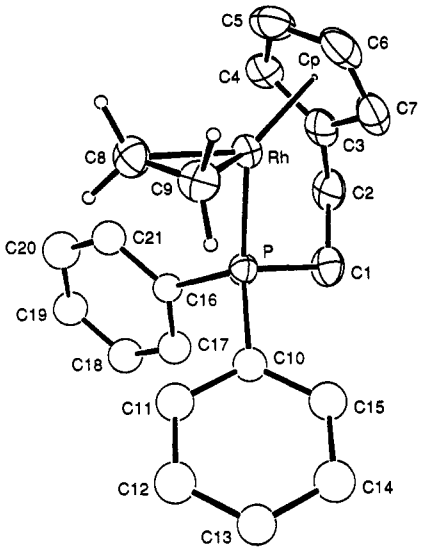

Figure 2. Perspective representation of the rhodium(I) complex $(\eta^5{:}\eta^1\text{-}C_5H_4(CH_2)_2PPh_2)Rh(C_2H_4)$ (14).

powder, was recrystallized in pentane, affording mostly stable crystals further identified by elemental analysis and in solution by ^{31}P and ^1H NMR.

The molecular structure of 14, determined by an X-ray diffraction study, is shown in Figure 2. It appears as a chelated variant of the classical $C_5R_5M(C_2H_4)L$ (R = H, CH_3; L = tertiary phosphine) cyclopentadienyl derivatives.[18]

A significant observation was that no reaction was observed by bubbling carbon monoxide in a solution of 12 or 14, even at room temperature.

With the diolefinic starting materials 4 and 5, preliminary NMR studies are related below. Interestingly, for both $(\eta^5\text{-}C_5H_4(CH_2)_2PPh_2)Rh(C_8H_{12})$ (15) and $(\eta^5\text{-}C_5H_4\text{-}(CH_2)_2PPh_2)Ir(C_8H_{12})$ (16) the ^{31}P NMR spectra exhibit singlets at δ −16.66 and −16.14, respectively. The latter shift is clearly indicative of a noncoordinated tertiary phosphine, as already observed in the derivatives of cyclopentadienyldiphenylphosphine.[2i]

Synthesis of Diiodorhodium(III) Chelate Complexes. Oxidative-addition reactions of iodine well-known to afford diiodorhodium(III) and -iridium(III) complexes would open in the present case an interesting access to numerous new chelated compounds.

Adding a CH_2Cl_2 solution of iodine to the carbonyl complex 8 in the same solvent led rapidly at room temperature to a maroon solution from which a powder analyzed as $(\eta^5{:}\eta^1\text{-}C_5H_4(CH_2)_2PPh_2)RhI_2$ (17) was obtained. Red-brown crystals were then obtained by slow diffusion of diethyl ether into a saturated CH_2Cl_2 solution of 17. The molecular structure of 17 determined by X-ray diffraction is shown in Figure 3 and will be discussed below.

In iridium chemistry, the ethylene complex 12 was chosen as starting material with the similar purpose of preparing the corresponding diiodoiridium(III) compound. The reaction was performed at room temperature in CH_2Cl_2 and after 1 h afforded only the diiodo compound 18, which was fully identified by its $^{31}P\{^1H\}$ NMR spectra.

Crystal and Molecular Structures of the Chelated Compounds $(\eta^5{:}\eta^1\text{-}C_5H_4(CH_2)_2PPh_2)Rh^I(C_2H_4)$ (14) and $(\eta^5{:}\eta^1\text{-}C_5H_4(CH_2)_2PPh_2)Rh^{III}I_2$ (17). In the chelation of

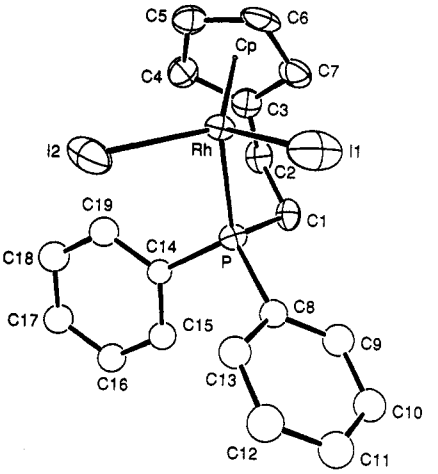

Figure 3. Perspective representation of the rhodium(III) complex $(\eta^5{:}\eta^1\text{-}C_5H_4(CH_2)_2PPh_2)RhI_2$ (17).

the (cyclopentadienylethyl)diphenylphosphine ligand in compounds 8, 11, and 13–18 the question arose of the occurrence of specific deformations of the coordination polyhedra around the metal center and of the arrangement of the (ethyl)diphenylphosphine arm. Therefore, crystallographic investigations of suitable crystals of 14 and 17 were carried out. This type of structure has already been exemplified by the X-ray investigations of ((dialkylphosphino)cyclopentadienyl)ruthenium[3a] and ((dialkylphosphino)-2,3,4,5-tetramethylcyclopentadienyl)cobalt[3c] derivatives as well as by ((dialkylamino)cyclopentadienyl)molybdenum[5b] and ((dialkylamino)-2,3,4,5-tetramethylcyclopentadienyl)cobalt[4a] derivatives.

Figures 2 and 3 show ORTEP views[13] of 14 and 17, while selected bond lengths and angles are given in Tables 6 and 7.

In both cases, the molecular structures built from similar $(\eta^5{:}\eta^1\text{-}C_5H_4(CH_2)_2PPh_2)Rh$ fragments offer a largely open space for coordination either with the η^2-ethylene ligand in 14 or with two iodide ligands in 17.

In the absence of any type of constraint arising from steric hindrance or from covalent bonding directivity, these molecules should have the Cp–Rh–P plane (Cp is the centroid of the cyclopentadienyl ring) as a mirror plane. Therefore, the various distortions from this ideal symmetry can be visualized as deviations from this plane (Table 8). Thus, as already noticed in analogous cases,[4a,5a,b,d] the C(3)–C(2)–C(1)–P chains in both compounds 14 and 17 deviate from planarity. The overall distortion can be described as resulting not only from this expected nonplanar configuration of the chelating chain but also from a restricted rotation of the phosphine around the Rh–P axis relative to the $\eta^5\text{-}C_5H_4(CH_2)_2Rh(C_2H_4)$ or $\eta^5\text{-}C_5H_4\text{-}(CH)_2RhI_2$ fragment. Therefore, both 14 and 17 adopt enantiomeric forms which in the $P2_1/n$ crystallographic unit cells are connected by centrosymmetrical operations. This description implies that the enantiomeric forms not only differ in the inversion of the Rh–P–CH_2–CH_2–C_5H_4 ring but also in the angular location of the phosphine group around the Rh–P axis.

An additional feature of the molecular structures that deserves comment is the coordination of the cyclopentadienyl rings. In both 14 and 17, the cyclopentadienyl rings are kept planar (Table 9), within an acceptable approximation, but the above-described conformations are associated with significant tilts of these rings, which favor

(18) Guggenberger, L. J.; Cramer, R. *J. Am. Chem. Soc.* **1972**, *94*, 3779–3786.

Table 6. Selected Bond Lengths (Å) and Angles (deg) with Esd's in Parentheses for 14

	molecule A	molecule B
Rh–Cp	1.896(6)	1.889(6)
Rh–P	2.189(1)	2.190(2)
Rh–C(3)	2.140(6)	2.155(5)
Rh–C(4)	2.245(5)	2.254(6)
Rh–C(5)	2.288(5)	2.286(6)
Rh–C(6)	2.297(5)	2.284(5)
Rh–C(7)	2.247(6)	2.233(5)
Rh–C(8)	2.101(6)	2.110(6)
Rh–C(9)	2.114(6)	2.102(6)
P–C(1)	1.843(5)	1.857(5)
P–C(10)	1.821(4)	1.835(4)
P–C(16)	1.830(4)	1.834(4)
C(1)–C(2)	1.524(8)	1.512(8)
C(2)–C(3)	1.516(8)	1.504(8)
C(3)–C(4)	1.420(8)	1.438(8)
C(4)–C(5)	1.408(9)	1.397(8)
C(5)–C(6)	1.404(9)	1.436(8)
C(6)–C(7)	1.408(9)	1.397(9)
C(7)–C(3)	1.420(8)	1.438(8)
C(8)–C(9)	1.402(9)	1.376(8)
Cp–Rh–P	118.5(2)	118.6(2)
Cp–Rh–C(8)	139.8(2)	140.2(3)
Cp–Rh–C(9)	137.7(2)	138.1(2)
P–Rh–C(8)	97.7(2)	96.9(2)
P–Rh–C(9)	98.4(1)	98.8(2)
C(8)–Rh–C(9)	38.8(2)	38.1(2)
Rh–P–C(1)	102.7(2)	102.3(2)
Rh–P–C(10)	120.7(1)	122.2(1)
Rh–P–C(16)	119.5(1)	118.6(1)
C(1)–P–C(10)	106.4(2)	105.3(2)
C(1)–P–C(16)	102.6(2)	102.9(2)
C(10)–P–C(16)	102.9(2)	103.3(2)
C(9)–C(8)–C1(C8)	122(2)	121(3)
C(9)–C(8)–H2(C8)	118(3)	121(2)
H1(C8)–C(8)–H2(C8)	108(4)	114(4)
C(8)–C(9)–H1(C9)	114(3)	118(3)
C(8)–C(9)–H2(C9)	123(3)	125(2)
H1(C9)–C(9)–H2(C9)	115(4)	112(4)
P–C(1)–C(2)	106.8(4)	107.4(4)
C(1)–C(2)–C(3)	111.0(5)	111.2(4)
C(7)–C(3)–C(4)	107.9(5)	106.8(5)
C(3)–C(4)–C(5)	107.2(5)	108.3(5)
C(4)–C(5)–C(6)	108.7(6)	108.2(5)
C(5)–C(6)–C(7)	108.2(5)	108.2(5)
C(6)–C(7)–C(3)	107.6(5)	108.3(5)
C(2)–C(3)–C(7)	125.2(5)	127.8(5)
C(2)–C(3)–C(4)	126.9(5)	125.4(5)

shorter Rh–C distances for C(3) in 14 (Table 6) and for C(3) and then C(4) and C(7) in 17 (Table 7). Moreover, in 17, the two iodo ligands are not symmetrically located *versus* the Cp–Rh–P plane (Table 8); their angular location around the Rh–P axis reveals their tendency to occupy the free space as it is shaped by the positions of the methylene groups of the C(3)–C(2)–C(1)–P chains.

MO calculations[17] have shown that bending of complexes by chelate ligands must lead to increased reactivity of the corresponding fragment, and it was also interesting to compare from this point of view the present structures of 14 and 17, respectively, with those of similar but nonchelated compounds. Several examples of molecular structures of $(\eta^5\text{-}C_5R_5)RhL(C_2H_4)$ complexes (R = H, L = C_2F_4,[18] and C_2H_4;[19] R = Me, L = PPh_3[20]) as well as of their iridium analogues $(\eta^5\text{-}C_5R_5)IrL(CO)$ (R = H, L = PPh_3;[21] R = Me, L = CO[22]) have been described. Compound 14 may be compared with the structurally analogous complex

(19) Blom, R.; Rankin, D. W. H.; Robertson, H. E.; Perutz, R. N. *J. Chem. Soc., Dalton Trans.* **1993**, 1983–1986.
(20) Porzio, W.; Zocchi, M. *J. Am. Chem. Soc.* **1978**, *100*, 2048–2052.
(21) Bennett, M. J.; Pratt, J. L.; Tuggle, R. M. *Inorg. Chem.* **1974**, *13*, 2408–2413.

Table 7. Selected Bond Lengths (Å) and Angles (deg) with Esd's in Parentheses for 17

Rh–I(1)	2.654(1)	Rh–P	2.267(2)
Rh–I(2)	2.6683(8)	Rh–Cp	1.844(8)
C(1)–C(2)	1.510(11)	C(2)–C(3)	1.482(11)
C(3)–C(4)	1.422(12)	Rh–C(3)	2.143(7)
C(4)–C(5)	1.437(12)	Rh–C(4)	2.188(9)
C(5)–C(6)	1.390(13)	Rh–C(5)	2.251(9)
C(6)–C(7)	1.426(12)	Rh–C(6)	2.226(9)
C(7)–C(3)	1.438(12)	Rh–C(7)	2.124(8)
P–C(1)	1.850(8)		
P–C(8)	1.808(5)	P–C(14)	1.823(4)
I(1)–Rh–I(2)	93.30(2)	I(2)–Rh–P	95.67(5)
I(1)–Rh–P	94.29(5)	I(2)–Rh–Cp	127.7(3)
I(1)–Rh–Cp	121.0(3)	P–Rh–Cp	117.3(3)
C(1)–C(2)–C(3)	110.0(7)	P–C(1)–C(2)	106.7(5)
C(7)–C(3)–C(4)	105.7(7)	C(3)–C(4)–C(5)	109.4(7)
C(4)–C(5)–C(6)	107.4(8)	C(5)–C(6)–C(7)	108.8(8)
C(6)–C(7)–C(3)	108.7(8)		
C(2)–C(3)–C(7)	126.2(7)	C(2)–C(3)–C(4)	127.8(7)
Rh–P–C(1)	99.7(3)	C(1)–P–C(8)	107.4(3)
Rh–P–C(8)	122.9(2)	C(1)–P–C(14)	103.3(3)
Rh–P–C(14)	117.3(2)	C(8)–P–C(14)	104.2(2)

Table 8. Deviations (Å) from the Plane Cp–Rh–P for 14 and 17

	14		
	molecule A	molecule B	17
Cp	0.000(6)	0.000(6)	0.000(9)
Rh	0.0000(4)	0.0000(5)	0.0000(5)
P	0.000(1)	0.000(1)	0.000(2)
C(1)	–0.479(6)	0.575(5)	–0.724(8)
C(2)	0.267(6)	–0.111(5)	0.006(8)
C(3)	0.129(6)	–0.035(5)	0.011(8)
C(4)	1.183(6)	–1.164(6)	1.136(9)
C(5)	0.592(6)	–0.690(6)	0.687(9)
C(6)	–0.804(6)	0.745(6)	–0.70(1)
C(7)	–1.100(6)	1.144(6)	–1.141(9)
C(8)	0.643(6)	–0.676(6)	–2.0770(7) (I(1))
C(9)	–0.758(6)	0.698(6)	1.7788(7) (I(2))

Table 9. Deviations (Å) from the Cyclopentadienyl Plane for 14 and 17

	14		
	molecule A	molecule B	17
C(3)	–0.031(5)	0.026(5)	–0.007(7)
C(4)	0.026(5)	–0.027(6)	0.001(8)
C(5)	–0.015(6)	0.015(6)	0.006(8)
C(6)	–0.009(6)	0.005(6)	–0.012(9)
C(7)	0.027(6)	–0.023(6)	0.011(8)
Rh	–1.8913(4)	1.8845(5)	1.8174(6)
C(1)	–1.381(5)	1.400(5)	1.313(8)
C(2)	–0.151(6)	0.148(5)	0.089(8)

$(\eta^5\text{-}C_5Me_5)RhPPh_3(C_2H_4)$.[20] The most significant effect brought about by the chelation appears effectively in the decrease of the Cp–Rh–P angle from 133.9(2)°[23] in the nonchelated species to 118.5(2)° in 14. Therefore, we are now trying to determine whether this variation of the bond hybridization of the rhodium atom leads to an increase of the reactivity of the (cyclopentadienylphosphine)rhodium fragment.

Finally it is tempting to compare[26] the change of the Rh–P distance to the change of the Rh–Cp distance on going from Rh(I) in 14 to Rh(III) in 17. The first distance

(22) Chen, J.; Daniels, L. M.; Angelici, R. J. *Acta Crystallogr.* **1993**, *C49*, 1061–1063.
(23) Value recalculated from ref 19.

Chart 1

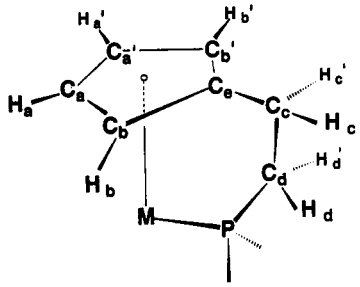

increases as the latter decreases, a fact which probably correlates with the softness of the phosphine ligand, which is able to bond more strongly with Rh(I) than with Rh(III), and with the anionic character of the cyclopentadienyl group, which is able to bond more strongly with Rh(III) than with Rh(I). Under such conditions, the metal atom finds its best fitting position between its two ligands.

Further NMR Observations. In contrast with the crystalline structures described above, ^1H and ^{13}C NMR experiments are unambiguously consistent with the existence of an apparent plane of symmetry in the carbonyl (8, 10), ethylene (13, 14), and diodide (17, 18) rhodium and iridium chelated complexes.

The ^1H NMR spectra (Table 5) consist in each case of two multiplets of equal intensities for the two sets of protons H_a and H_b of the cyclopentadienyl ring (see Chart 1) together with two doublets of triplets of equal intensities for the two sets of methylene protons H_c and H_d.

The equivalence of both H_c protons as well as that of both H_d protons is also supported by the multiplicity of their NMR signals (Table 5). Moreover, consideration of the methylene proton–phosphorus coupling constant values leads clearly to the assignation of lower and higher field methylene signals to H_d and H_c protons, respectively.

At this point of our investigations, the apparent planar symmetry observed by NMR in solution does contrast with the existence of the enantiomeric distorted from observed by X-ray diffraction in the crystals. Considering the molecular structures of **14** and **17** in the solid state as typical for the whole series of studied compounds, the ^1H NMR data clearly revealed the occurrence of a fluxional process. It is suggested that this dynamic process is an oscillation between the two enantiomeric distortions described above as the result of an inversion of the Rh–P–CH_2–CH_2–C_5H_4 ring coupled in **17** with an angular shift of the terminal ligands.

The ^{13}C NMR spectrum of the ethylene complex **14** exhibits the following resonances: two doublets of doublets of doublets centered at 87.82 ppm for C_a ($^1J_{C_aH_a}$ = 171.3 Hz; $^2J_{C_aRh}$ = 2.7 Hz; $^2J_{C_aP}$ = 9.0 Hz) and at 83.48 ppm for C_b ($^1J_{C_bH_b}$ = 173.8 Hz; $^2J_{C_bRh}$ = 3.3 Hz; $^2J_{C_bP}$ = 3.3 Hz); two doublets of triplets centered at 23.71 ppm for C_c ($^1J_{C_cH_c}$ = 129.2 Hz; $^2J_{C_cP}$ = 4.3 Hz) and at 49.84 ppm for C_d ($^1J_{C_dH_d}$ = 130.2 Hz; $^2J_{C_dP}$ = 29.4 Hz); a broad singlet at 112.60 ppm for C_e; a single doublet of doublets of triplets centered at 28.99 ppm for both ethylene carbons ($^1J_{CH}$ = 153.5 Hz; $^1J_{CRh}$ = 15.1 Hz; $^2J_{CP}$ = 1.9 Hz).

The magnetic equivalent of these ethylenic carbon atoms is again in agreement with the above dynamic process, for which a spectrum at the slow-exchange limit is easily obtained in ^{13}C NMR.

With regard to the ethylene protons, variable-temperature ^1H NMR experiment runs on a solution of **14** indicate the well-known internal hindered rotation of the ethylene ligand around the metal–ethylene bond.[24] Indeed, around 243 °C, two broad resonances respectively centered at 2.40 and 1.12 ppm, attributed to the pairs of nonequivalent protons, respectively, indicate that, at this temperature, the slow-exchange limit for the rotation has already been reached. When the temperature is lowered, these two signals transform into well-resolved multiplets interpretable as the A and M parts of a second-order AA'MM'XY spin system. When the internal rotation of ethylene is expressed in slow-exchange-limit spectra, *i.e.* at room temperature and below, the overall nonrigidity process described above still leads to fast-exchange signals. Therefore, the latter phenomenon occurring in the chelating species is a process of low activation energy similar to the comparable dynamic deformation in the bridged dinuclear derivative of the (diphenylphosphino)cyclopentadienyl ligand.[25] Simulations of these spectra in order to check the coupling constant values and to obtain kinetic parameters are in progress.

Supplementary Material Available: Listings of H atom parameters, anisotropic thermal parameters, all bond distances and angles, and least-squares planes and deviations therefrom for **17** and **14** (10 pages). Ordering information is given on any current masthead page.

OM940050A

(24) (a) Cramer, R. *J. Am. Chem. Soc.* **1964**, *86*, 217–221. (b) Cramer, R.; Kline, J. B.; Roberts, J. D. *J. Am. Chem. Soc.* **1969**, *91*, 2519–2525.

(25) Tommasino, J.-B.; de Montauzon, D.; He, X. D.; Maisonnat, A.; Poilblanc, R.; Verpeaux, J.-N.; Amatore, C. *Organometallics* **1992**, *11*, 4150–4156.

(26) We thank one of the reviewers for this suggestion.